

# Mechanisms Involved in Ceramide-Induced Autophagy in Osteoblasts

Nadia Abed Al-Hazmi<sup>1</sup>, Turki Yousef Alhazzazi<sup>1</sup>, Sahar Mohammed Nour Bukhary<sup>1</sup>, Daniel Weekes<sup>2</sup>, Fraser McDonald<sup>3</sup>, Peter Hill<sup>4</sup>, Agamemnon Grigoriadis<sup>4</sup>, Raghad Abdullah Al-Dabbagh<sup>5\*</sup>

<sup>1</sup>Department of Oral Biology, Faculty of Dentistry, King Abdulaziz University, Jeddah, Saudi Arabia. <sup>2</sup>The Institute of Cancer Research, London, Greater London, UK. <sup>3</sup>Department of Craniofacial and Regenerative Biology, Dental Institute, King's College London, London, UK. <sup>4</sup>Belmont Park Dental Care, Lewisham, London, UK. <sup>5</sup>Department of Oral and Maxillofacial Prosthodontics, Faculty of Dentistry, King Abdulaziz University, Jeddah, Saudi Arabia.

## Abstract

This study aimed to investigate the role of ceramide in inducing autophagy in osteoblasts, then further investigate the involved downstream signaling cascades. The effect of exogenous ceramide on inducing autophagy in MC3T3-E1 and Primary murine osteoblasts (POB) were assessed by (a) Transmission Electron Microscopy (TEM), Western Blot (WB) analysis, (c) Immunofluorescence microscopy, and (d) Propidium Iodide (PI)-uptake/flow cytometry analysis. C2-ceramide induced the formation of cytoplasmic vacuoles and elevated the expression of the autophagy proteins Atg5, beclin1, and LC3 II. Silencing Atg5 or beclin1 with siRNAs partially rescued the C2-ceramide-induced cell death in osteoblasts yet this silencing did not rescue the C2-ceramide-induced autophagy as assessed by TEM. Hence, these results suggest that C2-ceramide induces Atg5 and beclin1-independent autophagic cell death in osteoblasts. This work highlighted a novel role for ceramide in inducing autophagy in osteoblasts. The use of ceramide or inhibitors of its synthesis could be utilized as a therapeutic tool for modulating osteoblast survival in different metabolic bone diseases.

**Keywords:** Ceramide, Osteoblasts, Apoptosis, PCD, Signaling, MAPK

## INTRODUCTION

Cell and tissue homeostasis are maintained by tightly balanced catabolic and anabolic processes. In eukaryotes, degradation primarily occurs through the ubiquitin-proteasome system or lysosomes (endocytosis and autophagy). Autophagy mediates a tightly regulated self-eating process, by sequestering cytoplasm, organelles, and long-lived proteins for recycling [1]. Dysregulation is associated with diseases such as cancer, neurodegenerative diseases, and myopathies because the efficient removal of damaged organs is important for survival and normal function [2]. Several reports in the literature support the role of autophagy in health and disease [1-9].

However, only a few reports in the literature support a role for autophagy in bone; among them is a report that demonstrated the involvement of autophagy in chondrocyte survival during endochondral ossification. In this report, sulfatase modifying factor 1 (Sumf1), the activator of all sulfatases, knockdown mice were analyzed. Sumf1 was partially rescued by beclin1 silencing [10, 11]. In addition, others reported showed that hypertrophic chondrocytes were sensitized to hypoxia through the activation of autophagy. Sustained stress subsequently induced chondrocyte cell death which was partially rescued by beclin1 silencing [12]. Moreover, the involvement of autophagy in Paget's disease of bone (PDB) and osteosarcoma was reported [13, 14].

PDB is frequently associated with p62/sequestrome 1 (SQSTM1) mutations. This might suggest the involvement of p62 in inclusion body formation present in PDB [15].

Ceramides are the precursors to all complex sphingolipids. They are critical bioactive secondary messengers that play significant roles in several cell processes such cellular proliferation, differentiation, senescence, and programmed cell death (PCD) [16]. Ceramide and sphingosine 1-phosphate (S1P) are important mediators that balance the fate of cells between death and survival. Recently both have been reported to induce autophagy [17, 18]. However, the role of ceramide-induced autophagy and the molecular

**Address for correspondence:** Raghad Abdullah Al-Dabbagh, Department of Oral and Maxillofacial Prosthodontics, Faculty of Dentistry, King Abdulaziz University, Jeddah, Saudi Arabia. [raaldabbagh@kau.edu.sa](mailto:raaldabbagh@kau.edu.sa)

This is an open-access article distributed under the terms of the Creative Commons Attribution-Non-Commercial-Share Alike 4.0 License, which allows others to remix, tweak, and build upon the work non commercially, if the author is credited, and the new creations are licensed under the identical terms.

**How to cite this article:** Al-Hazmi NA, Alhazzazi TY, Bukhary SMN, Weekes D, McDonald F, Hill P, et al. Mechanisms Involved in Ceramide-Induced Autophagy in Osteoblasts. Arch Pharm Pract. 2021;12(3):125-33. <https://doi.org/10.51847/B8jiA53A5q>

events in osteoblasts have not been investigated. Thus, this study aimed to examine the role of ceramide in inducing autophagy in osteoblasts, then further explore the involved downstream signalling cascades.

## MATERIALS AND METHODS

### Reagents and Antibodies

The reagents were purchased from Sigma-Aldrich and Calbiochem (Nottingham, UK). The antibodies used were purchased from Cell Signalling, Alexa fluor 555 goat anti-rabbit IgG was purchased from Invitrogen (Paisley, UK) and Vectorshield mounting medium with DAPI was purchased from Vector laboratories Inc (Peterborough, UK).

### Cell Culture

The murine osteogenic cell line established from newborn mouse calvaria, MC3T3-E1 [19] was purchased from the Global Biosource Center (ATCC). Primary murine osteoblasts were isolated as described [20]. Briefly, neonatal calvariae were dissected clean from attached tissue and washed in Tyrode's solution (Sigma-Aldrich, UK). Then, calvariae were sequentially digested in 1 mg/ml trypsin for 10 minutes, 2 mg/ml of dispase II for 15 minutes, and 2 mg/ml of collagenase A for 30 minutes (repeated 3 times) (Roche Applied Science, Germany). Cells released by the three collagenase digestions were grown in medium and were ready for experiments next day. All cells were cultured in  $\alpha$ -minimum essential medium ( $\alpha$ -MEM) supplemented with 10% fetal bovine serum (Autogenbiochlear, Nottingham, UK), antibiotics (penicillin 50 units/ml, streptomycin 50  $\mu$ g/ml) and L-glutamine (5 mM) (Sigma-Aldrich, UK). All cultures were maintained at 37°C in a humidified atmosphere of 5% CO<sub>2</sub>. In accordance with the UK Home Office Project License P8D5E2773 (K.J.L.), all work was performed at King's College London.

### Mitochondrial Viability Assay (MTT)

Mitochondrial activity and viability were measured through the mitochondrial enzymatic activity where mitochondrial dehydrogenase (in viable cells) reduces the tetrazolium rings of the pale yellow MTT to dark blue formazan insoluble crystals. Osteoblasts were seeded in 96-well plates (Dutscher Scientific, UK) at 5 x 10<sup>3</sup> cells/well. After treatment with the reagents for the periods indicated, the medium was replaced with fresh 10% MTT (5mg/ml in PBS) containing medium and incubated for 5 hours at 37°C and 5% CO<sub>2</sub>. To solubilize the formazan crystals, MTT was washed with PBS and medium replaced with 1:1 isopropanol: PBS for 1 hour at room temperature in the dark. The optical density was measured with a microplate reader (Labsystems ELISA reader) using a reference wavelength of 620 nm and a test wavelength of 562 nm. Control wells represent cells with MTT containing medium only and blank wells represent MTT containing medium free cells.

### Transmission Electron Microscopy (TEM)

Cells were plated on 13 mm coverslips and were cultured as above. Then they were fixed in 2.5% glutaraldehyde for 3 hours at 4°C, washed, and stored in PBB (pH 7.3). Cells were post-fixed in 1% osmium tetroxide at 4°C for 15-30 minutes and then were dehydrated with ascending grades of ethyl alcohol. The dehydrated cells were embedded in TAAB premix medium resin which was left to polymerize for at least 24 hours. The resin blocks were then cut into ultra-thin sections with the Leica Ultra-machine and placed on 150 mesh Guilder grids. The grids were stained with a saturated Uranyl acetate solution and a 4% lead citrate solution for visualization with a Hitachi H7600 TEM (Tokyo, Japan).

### Analysis of PI-uptake by FACS Analysis

*In vitro* loss of plasma membrane integrity, which occurs in apoptotic cells, was assessed by PI-uptake. Cells were plated in 12-well plates (Dutscher Scientific, UK) at 10<sup>5</sup> cells/well. Cells were left to settle overnight and then were treated with the indicated reagents for the indicated periods. Then, cells were re-suspended in 1x binding buffer (BD Pharmingen) and incubated with 50  $\mu$ g/ml PI. At later stages of cell death, there is a loss of cytoplasmic integrity, facilitating PI cell and nuclear staining, which fluoresces red when excited at 510-550 nm. Healthy cells having an intact cytoplasmic membrane prevent PI entry and nuclear staining is hindered. Cells positive for PI (red) were considered as undergoing PCD. FACS analysis was performed immediately after staining where 10<sup>4</sup> cells were captured per condition with BD FACS CantoTM II flow cytometer and samples were analyzed with BD FACSDiva software. Results were expressed as the percentage of PI-uptake which were expressed as mean  $\pm$  standard error of the mean (SEM) of five replicas.

### Western Blot Analysis

Activation of MAPK members and various caspases and downstream targets were assessed at the protein level by Western blot analysis (WB). Cells were plated in 6-well plates (Dutscher Scientific, UK) at 2x10<sup>5</sup> cells/well. Cells were left to settle overnight and then were treated with the indicated reagents for the indicated periods. Experiments were terminated with PBS at 4°C and cells were lysed with lysis buffer (4.8% SDS, 8% sucrose, and 2M urea). Samples were spun through glass wool at 14000 x g, and supernatants were boiled for 3 minutes. Samples were added to 4x SDS-sample buffer and lysates were separated on 8-15% SDS-PAGE gels, and transferred onto polyvinylidene difluoride membranes (Millipore Corp., MA, USA). Primary and secondary antibodies were incubated at the concentrations and times indicated. Immunocomplexes were visualized by enhanced chemiluminescence according to the manufacturer's instructions (ECL; Amersham Pharmacia Biotech, UK).

### SiRNA Transfection

Atg5 and beclin1 were silenced by transfecting cells with siRNA (100 nM) using the cationic lipid DharmaFECT (2  $\mu$ l/well, ThermoFisher Scientific). Western blots assessed Seventy-two hours post-transfection, knockdown of the intended targets. Post transfection, cells were treated with the indicated reagents for the indicated concentrations and periods, and experiments were then stopped by detaching, lysing, or fixing cells depending on the type of analysis they will undergo. Cells destined for PI-uptake were detached by treatment with 0.25% trypsin for 3 minutes at 37°C. Cells were then pelleted in preparation for PI staining as detailed in section PI-uptake by FACS analysis section. Cells to be analyzed by WB were lysed as described in the Western blot analysis section and cells to be analyzed by TEM were fixed in 2.5% glutaraldehyde as described in the TEM section.

### Statistical Analysis

Mean  $\pm$  standard deviation (SD) from 5-7 replicas represented all data. Student *t*-test or ANOVA and Bonferroni tests were utilized to analyze the differences between controls and treated samples. Statistical significance was defined as \* $P < .05$ , \*\* $P < .01$ , and \*\*\* $P < .001$ . Experiments were repeated at least 3 times for verification.

## RESULTS AND DISCUSSION

### Exogenous Ceramide Induces the Formation of Autophagic Compartments in Osteoblasts

Fluorescent microscopy revealed that cells treated for 24 and 48 hours showed nuclear changes atypical of apoptosis (**Figure 1a**). The ultra-structural changes were then assessed for MC3T3-E1 cells after C<sub>2</sub>-ceramide treatment. Transmission electron microscopy (TEM) revealed that cells treated for 6 hours started to show cytoplasmic vacuolization which increased with a prolonged incubation period (**Figure 1b**). At the short incubation period (6 hours), cells showed no signs of nuclear changes, however, cytoplasmic blebbing was apparent, a characteristic of apoptosis (**Figure 1be**) (red arrowheads). In contrast, cells treated with staurosporine for only 3 hours, showed nuclear margination (chromatin is marginated towards the nuclear membrane) and signs of chromatin condensation (**Figure 1bk**) (red arrows). At 12 hours of treatment, early signs of apoptosis were emerging; nuclear margination and cytoplasmic blebbing (**Figure 1be**) (red arrows, and arrowheads). In addition, the cytoplasmic vacuoles were more apparent, and a mixture of double and single-membrane compartments was obvious (**Figure 1bf**) (blue arrows, and arrowheads). Thus, this confirms that C<sub>2</sub>-ceramide induces a slow apoptotic process in osteoblasts. At 24 hours of treatment, C<sub>2</sub>-ceramide further enhanced the formation of large vacuoles resulting in the consumption of the cytoplasm (**Figure 1bh**) (blue arrows). The vesicles formed resembled those generated due to chloroquine treatment (single-membrane structures) (**Figure 1bn**), (blue arrows), however, the vesicular content (cytosol and

organelles) was less in the C<sub>2</sub>-ceramide treated cells (**Figure 1bh**), (blue arrows). Chloroquine is known to disrupt lysosomal structure and function preventing effective autophagic degradation, leading to the accumulation of ineffective autolysosomes [21]. C<sub>2</sub>-DHC treated cells showed no nuclear nor cytoplasmic changes indicative of the selectivity of the C<sub>2</sub>-ceramide-induced effects. This was confirmed by quantitative electron microscopy which showed a significant increase of early autophagic vacuoles (EAV) and late autophagic vacuoles (LAV) at 12 and 24 hours of treatment, respectively (**Figure 1c**).

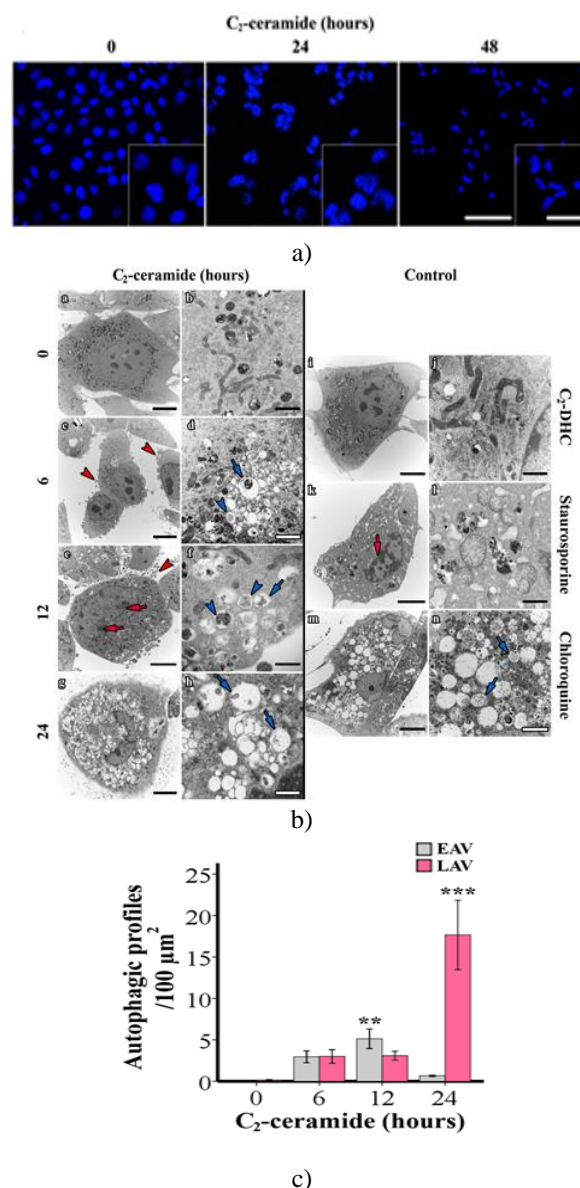


**Figure 1.** C<sub>2</sub>-ceramide-induced apoptosis is associated with an increased formation of cytoplasmic compartments in MC3T3-E1 cells.

(a) MC3T3-E1 cells were treated with vehicle or a C<sub>2</sub>-ceramide (100  $\mu$ M) for the indicated periods and nuclear morphology was assessed. Cells were stained with Hoechst 33324 and visualized using fluorescent microscopy.

Images are taken from representative fields. Scale bars are 50 and 12.5  $\mu\text{m}$  in length, (b) Ultrastructural changes were assessed by TEM. MC3T3-E1 cells were treated with C<sub>2</sub>-ceramide (100  $\mu\text{M}$ ). MC3T3-E1 cells were treated with C<sub>2</sub>-ceramide (100  $\mu\text{M}$ ) for the indicated time points, C<sub>2</sub>-DHC (100  $\mu\text{M}$ ) for 24 hours, staurosporine (10  $\mu\text{M}$ ) for 3 hours, or chloroquine (10  $\mu\text{M}$ ) for 6 hours. Arrows represent cytoplasmic blebbing (red arrowheads), nuclear margination (red arrows), EAV (blue arrowheads), and LAV (blue arrows). (c) The amounts of EAV and LAV were determined by quantitative electron microscopy. C<sub>2</sub>-ceramide time-dependently increased the number of EAV and LAV (ANOVA; \* $P < 0.05$  and \* $P < 0.01$ ). Bonferroni test showed a significant difference from respective controls at \*\* $P < 0.01$  and \*\*\* $P < 0.001$ . Images are taken from representative fields.

C<sub>2</sub>-ceramide induced a dose-dependent increase in Atg5, beclin1, and LC3-II expression (Figure 2a). In addition, C<sub>2</sub>-ceramide induced a time-dependent increase in the conversion of LC3-I to LC3-II (Figure 2b). However, the upregulation of Atg5 and Beclin 1 expression in response to C<sub>2</sub>-ceramide treatment was maximal after 10 minutes and returned gradually to basal levels by 24 hours (Figure 2b). Next, to assess the effects of C<sub>2</sub>-ceramide on endogenous LC3 localization, MC3T3-E1 cells were treated with C<sub>2</sub>-ceramide, and effects were assessed by immunofluorescence and confocal microscopy. C<sub>2</sub>-ceramide induced an increase in the formation of punctuating LC3 compared to control cultures, which represents lipidated LC3 (LC3-II) co-localized at autophagocytic structures (Figure 2c). These accumulative results suggest that C<sub>2</sub>-ceramide increases the formation of autophagic structures in osteoblasts.

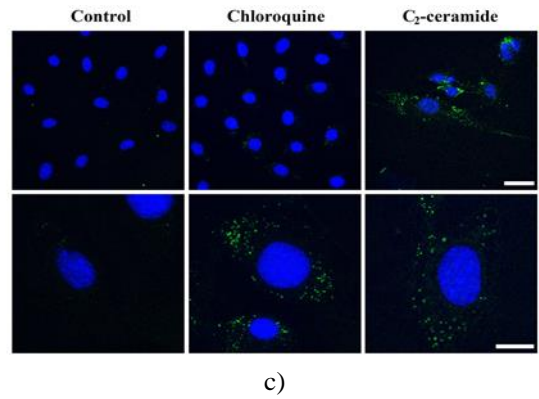
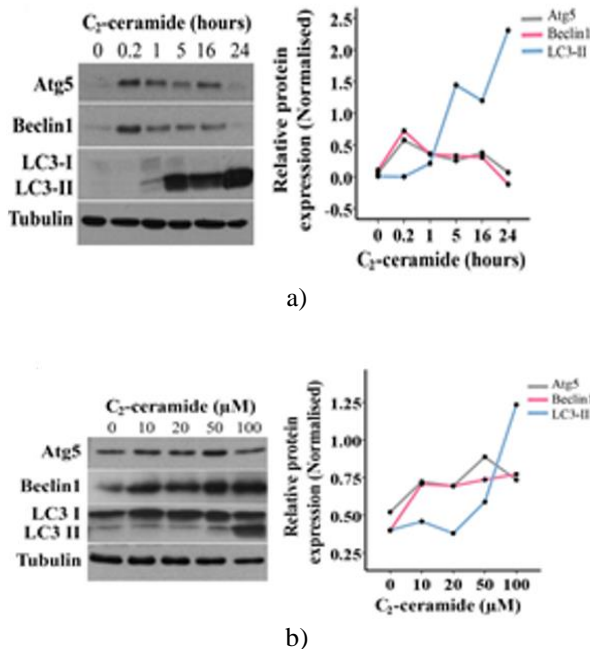


**Figure 2.** C<sub>2</sub>-ceramide dose and time-dependently up-regulates Atg5, beclin1, and LC3 expression in MC3T3-E1 cells.

(a) MC3T3-E1 cells were treated with C<sub>2</sub>-ceramide for 5 hours at the indicated concentrations or (b) with C<sub>2</sub>-ceramide (100  $\mu\text{M}$ ) for the indicated time points. Effects on expression of Atg proteins were assessed by Western blotting (right panel) and densitometric analysis of the blots (left panel) (c) Effects of C<sub>2</sub>-ceramide on the localization of LC3-II were assessed by fluorescent microscopy. Vehicle or C<sub>2</sub>-ceramide (100  $\mu\text{M}$ ) for 24 hours or chloroquine (10  $\mu\text{M}$ ) for 3 hours. Images are taken from representative fields. Scale bars are 150 and 50  $\mu\text{m}$  in length.

### Exogenous Ceramide Induces Autophagy in Osteoblasts

The effect of C<sub>2</sub>-ceramide on autophagic flux was determined by treating MC3T3-E1 cells with C<sub>2</sub>-ceramide for 24 hours in the presence and absence of PIs and assessing LC3-II levels by Western blot analysis. In the absence of the lysosomal PI, C<sub>2</sub>-ceramide produced a time-dependent increase in endogenous levels of LC3-II between 10 minutes and 5 hours (Figure 3a). The increase in LC3-II indicates that ceramide induces an increase in the accumulation of autophagosomes but does not guarantee autophagic degradation. Inclusion of the lysosomal PIs dramatically increased LC3-II levels in a time-dependent manner indicating a block of the autophagic flux. These results suggest that inhibiting lysosomal enzymes blocks the recycling of C<sub>2</sub>-ceramide-induced LC3 lipidation. However, the autophagic turnover process-induced is slow, and to assess when and if LC3-II levels return to basal levels, analysis of later time points is needed. In the absence of lysosomal PIs, C<sub>2</sub>-ceramide induced a non-significant increase in electron-dense double-membrane structures corresponding to EAV as early as 1 hour (Figure 3bf), (arrowheads), increasing significantly after 5 hours of treatment. Though, the structures formed were a combination of single- and double-membranes compartments (Figure 3bn), (arrow and arrowheads), representing LAV and EAV, respectively. This suggests that C<sub>2</sub>-ceramide induces the formation of autophagocytic structures in osteoblasts that show evidence of maturation as early as 5 hours of treatment. However, in the presence of lysosomal PIs, C<sub>2</sub>-ceramide induced a significant increase in

the number of EAV formed 5 hours, but not in 1 hour, compared to the C<sub>2</sub>-ceramide treated cultures without PIs. Yet, the formed structures were mostly EAV with the absence of LAV (Figures 3bh and 3bp); (arrowheads and arrow). This was confirmed by quantitative electron microscopy which showed that C<sub>2</sub>-ceramide significantly increased EAV and LAV at 5 hours of treatment (Figure 3b), (right panel). Pre-treatment with PIs significantly reduced the number of LAV and significantly increased the number of EAV (Figure 3b), (right panel) Thus, these results suggest that inhibiting lysosomal hydrolases increases the C<sub>2</sub>-ceramide-induced autophagocytic structures with the block in their maturation. Because of the presence of mature autophagocytic structures that contain digested cytoplasmic contents in C<sub>2</sub>-ceramide treated osteoblasts (Figure 3bn), (arrow), it is reasonable to conclude that this increase in vesicles number is due to induction in autophagy and not due to a block in turnover.

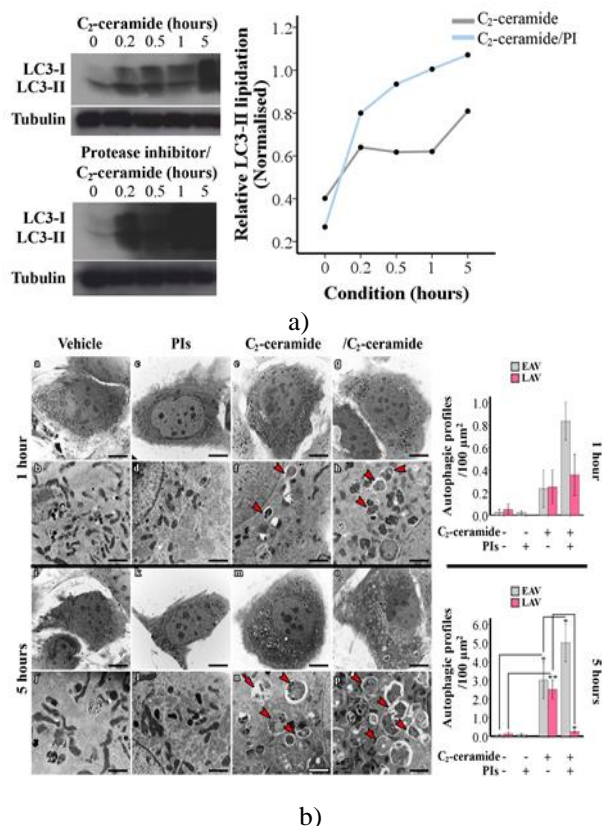


**Figure 3.** Protease inhibitors stabilize C<sub>2</sub>-ceramide-induced LC3-II upregulation and increase the C<sub>2</sub>-ceramide-induced formation of autophagosomes with a block in their maturation.

(a) MC3T3-E1 cells were pre-treated with PIs (10 μM) for 2 hours and then C<sub>2</sub>-ceramide (50 μM) at the indicated time points. Effects on LC3 lipidation were assessed by Western blotting followed by densitometric analysis. (b) Ultrastructural changes were assessed by TEM (left panel) and the amounts of EAV and LAV were determined by quantitative electron microscopy (right panel). Arrows represent EAV (arrowheads) and

LAV (arrow). At 1 hour, C<sub>2</sub>-ceramide and PIs non-significantly increased the number of EAV and LAV as compared to controls (\*P > 0.05). However, at 5 hours C<sub>2</sub>-ceramide significantly increased the number of EAV and LAV (\*P < 0.05 and \*\*P < 0.0). Furthermore, PIs significantly increased the number of EAV and significantly reduced the number of LAV as compared to C<sub>2</sub>-ceramide treated cells (\*P < 0.05). Images are taken from representative fields.

### Exogenous Ceramide Induces Autophagy Gene-Dependent Cell Death and Alternative Autophagy in Osteoblasts

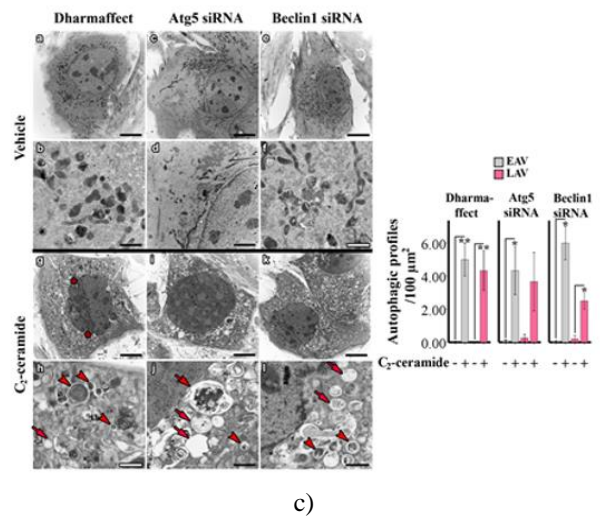
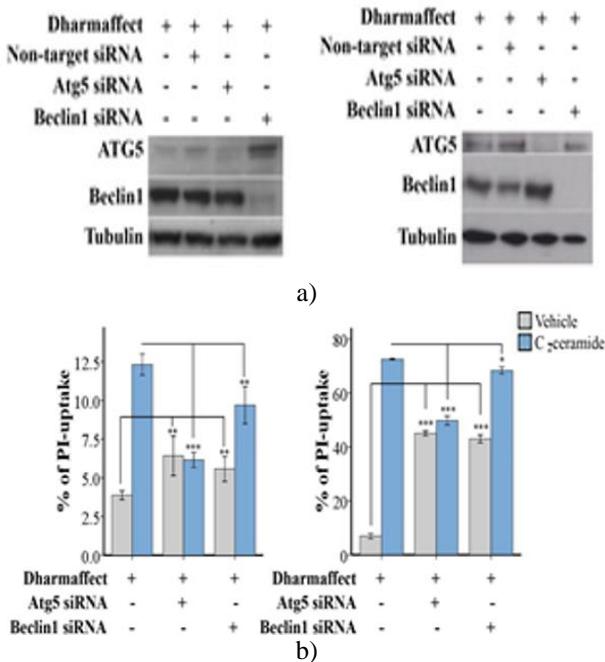
Unwarranted side effects of drugs endowed with limited selectivity may affect the autophagy pharmacological inhibition. Therefore, a siRNA approach was used to knock down Atg genes implicated in the autophagic pathway. First, the Beclin 1/Atg6 gene was targeted. A siRNA construct designed to down-regulate the expression of Beclin 1 reduced the expression of Beclin 1 protein in both MC3T3-E1 and POBs compared to a non-target siRNA control (Figure 4a). In the absence of C<sub>2</sub>-ceramide, this manipulation significantly increased the percentage of MC3T3-E1 cells and POBs that were PI-positive (Figure 4b). Whereas, in the presence of C<sub>2</sub>-ceramide, siRNA of beclin1 produced a slight but significant inhibition in C<sub>2</sub>-ceramide mediated osteoblast cell death (Figure 4b). Since beclin1 has been revealed to interact with bcl-2 [22], it may have been possible that the beclin1 effects involved direct crosstalk with mitochondria. Therefore, a siRNA construct designed to target the Atg5 gene was used. The siRNA construct designed to down-regulate the expression of Atg5 (Figure 4a) produced a similar increase in PI-positive MC3T3-E1 cells and POBs to that was seen with siRNA of beclin1 in the absence of C<sub>2</sub>-ceramide (Figure 4b). However, in the presence of C<sub>2</sub>-ceramide, Atg5 siRNA produced a more significant inhibition in cell death than that seen with beclin1 siRNA (Figure 4b). Thus, these siRNA experiments demonstrate a cytoprotective potential of autophagy on osteoblasts under resting conditions, whilst under conditions of C<sub>2</sub>-ceramide upregulation, autophagy would seem to contribute to the apoptotic cell death.

To further assess the effects of silencing Atg5 and beclin1 on C<sub>2</sub>-ceramide-induced autophagic compartment formation and autophagy, MC3T3-E1 cells were transfected with siRNA to Atg5 or beclin1 and ultrastructural changes were assessed by TEM. C<sub>2</sub>-ceramide increased the number of small double-membrane compartments containing subcellular constituents and single-membrane compartments in cells treated with transfecting reagent when compared to controls (Figure 4ch), (arrowheads and arrows). Furthermore, C<sub>2</sub>-ceramide induced early signs of nuclear margination in these cultures (Figure 4cg), (asterisks). Silencing Atg5 or beclin1 had no apparent effect on the C<sub>2</sub>-ceramide-induced increase in the number of both EAV and LAV (Figures 4cj and 4cl), (arrowheads and arrows) which was confirmed by quantitative electron microscopy (Figure

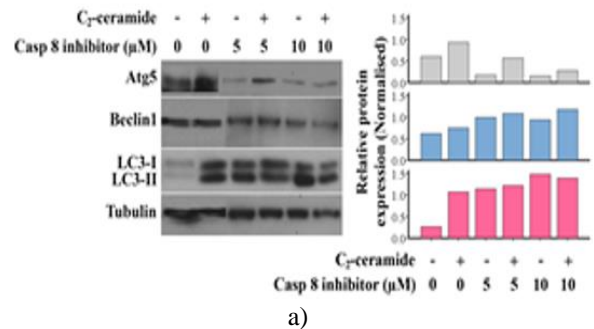
4c), (right panel). Additionally, C<sub>2</sub>-ceramide still induced upregulation of lipidated LC3 when Atg5 or beclin1 were silenced (data not shown). Thus, this suggests that C<sub>2</sub>-ceramide induces a non-canonical form of autophagy that is independent of Atg5 or beclin1 in osteoblasts.

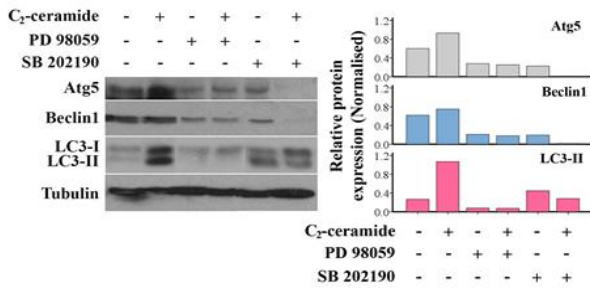
### Exogenous Ceramide Induced Caspase 8 and MAPK-Dependent Upregulation of Autophagy Proteins

To assess if caspase 8 was an effector in the C<sub>2</sub>-ceramide-induced autophagy, cells were pre-treated with a cell-permeable caspase-8 inhibitor I (IETD-CHO), and the effect on autophagy protein expression was assessed with Western blots. Caspase 8 inhibitor reduced basal and C<sub>2</sub>-ceramide-induced upregulation of Atg5 (**Figure 5a**). Finally, to further elucidate other molecular events, we previously demonstrated that C<sub>2</sub>-ceramide induced p38 and ERK phosphorylation, but that only p38 activation was part of the induced apoptotic pathway. To assess whether MAPK is an effector in C<sub>2</sub>-ceramide induced autophagy, MC3T3-E1 cells were pre-treated with a potent cell-permeable inhibitor of p38 MAPK (SB 202190), and a selective cell-permeable inhibitor of MEK (PD 98059). Western blot analysis showed both MAPK inhibitors reduced basal and C<sub>2</sub>-ceramide-induced Atg5, beclin1, and LC3-II upregulation (**Figure 5b**). Thus, caspase 8, p38, and ERK are possible effectors in basal and C<sub>2</sub>-ceramide-induced autophagy in osteoblasts.



**Figure 4.** Constitutive and C<sub>2</sub>-ceramide-stimulated Atg5 and beclin1 are survival and death effectors, respectively and C<sub>2</sub>-ceramide induced Atg5 and beclin1-independent autophagic compartments formation in osteoblasts. (a and b) MC3T3-E1 cells (left panels) and POB (right panels) were transfected or not (Dharmafect, transfection reagent only) with Atg5 and beclin1 siRNA for 3 days and treated with vehicle or C<sub>2</sub>-ceramide (50 or 100 μM) for 24 hours. (a) The efficiency of transfection was assessed by WB analysis. (b) Effects of PI-uptake were assessed by PI staining/flow cytometry. Silencing basal Atg5 or beclin1 sensitized osteoblasts to cell death (\*\*P < 0.01 and P < 0.001 (\*\*\*)). However, silencing C<sub>2</sub>-ceramide-induced Atg5 and beclin1 upregulation augmented C<sub>2</sub>-ceramide-induced osteoblast cell death (\*P < 0.05; \*\*P < 0.01 and P < 0.001 (\*\*\*)). (c) MC3T3-E1 cells were transfected or not (Dharmafect) with Atg5 siRNA or beclin1 siRNA in the presence of vehicle or C<sub>2</sub>-ceramide (50 μM) for 24 hours. Ultrastructural changes were assessed by TEM. Arrows represent: EAV (arrowheads), LAV (arrows) and nuclear margination (stars). The amounts of EAV and LAV were determined by quantitative electron microscopy. Silencing Atg5 and beclin1 did not rescue the ceramide induced increase in EAV and LAV (\*\*P < 0.001). Images are taken from representative fields.





b)

**Figure 5.** MAPK inhibitors reduce the C<sub>2</sub>-ceramide induced upregulation of autophagy proteins.

MC3T3-E1 cells were pre-treated with (a) Caspase 8 inhibitor, (b) PD98059 (20 μM) or SB202199 (10 μM) for 2 hour and C<sub>2</sub>-ceramide (50 μM) for 1 hour. Effect of inhibitors on C<sub>2</sub>-ceramide-induced upregulation of Atg5, beclin1, and LC3-II was assessed by WB (right panel) and densitometry (left panel).

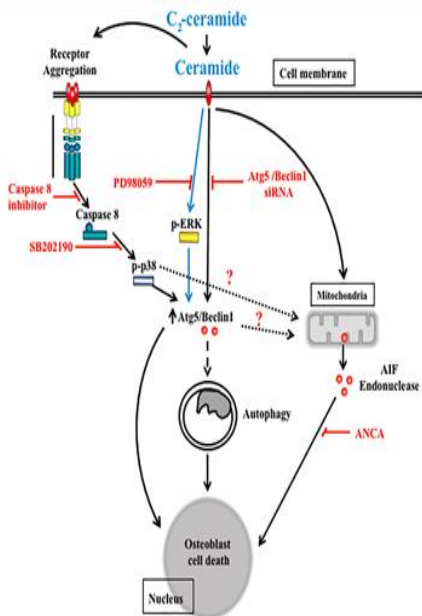


**Figure 6.** Proposed model of C<sub>2</sub>-ceramide-induced autophagy associated cell death in osteoblasts

Autophagy has been linked to bone diseases associated with high turnover such as osteosarcoma and Paget’s disease of bone [13, 14]. Ceramide and sphingosine 1-phosphate are important mediators that balance the fate of cells between death and survival. Ceramide is a pro-death molecule, while S1P is a pro-survival lipid and recently, both have been reported to induce autophagy [17]. However, the role of ceramide in inducing autophagy in osteoblasts and the molecular signalling cascades taking place have not been well investigated.

In this report, C<sub>2</sub>-ceramide induced autophagy-associated cell death in osteoblasts. Our results agree with other reports in different cell types such as malignant glioma cells and

human colon cancer cells [18, 23]. Daido *et al.* [23] have shown that in 24 hours of C<sub>2</sub>-ceramide treatment, extensive formation of autophagic vesicles was noticed and were mostly mature autophagosomes (autolysosomes). This was like our observation in osteoblasts where at 24 hours of treatment, the cytoplasm was consumed by these autolysosomes. Moreover, Park *et al.* [24] have shown that elevated endogenous levels of ceramide by combined treatment of sorafenib and vorinostat (anti-tumor reagents), induced cell death associated with autophagy in hepatocellular carcinoma and renal cell carcinoma cells. They also demonstrated that the combined treatment of sorafenib and vorinostat resulted in upregulated Atg5 expression and LC3 lipidation in a time-dependent manner yet, had no effect on beclin1 expression. In our report, C<sub>2</sub>-ceramide consistently induced a time-dependent increase in LC3 lipidation up to 24 hours of treatment just like sorafenib and vorinostat treatment. However, C<sub>2</sub>-ceramide upregulated Atg5 and beclin1 after 10 minutes of treatment and then these levels gradually subsided to basal and sub-basal levels between 1 and 24 hours of treatment. This could be explained, in part, by the possibility that sorafenib and vorinostat induced autophagy through other mechanisms other than elevating ceramide levels which lead to this sustained upregulation of Atg5 and beclin1 expression at 24 hours. Another possibility is the inherent differences between the cells investigated in these two reports.

The C<sub>2</sub>-ceramide induced autophagic compartment formation was attributed to autophagy induction, not due to vesicle turnover inhibition. During autophagy, lysosomal hydrolases degrade intra-autophagosomal components, following the formation of autophagosomes and their fusion with lysosomes to form autolysosomes. Therefore, lysosomal hydrolases may rapidly degrade a significant amount of LC3-II on autophagosomes. This was assessed by pre-treatment with protease inhibitors and then assessing effects of C<sub>2</sub>-ceramide induced LC3 lipidation (temporal dynamics) by WB and C<sub>2</sub>-ceramide induced formation of autophagic compartments by TEM. As mentioned earlier, the induction of autophagy resulted in transforming LC3-I (cytoplasmic form) to LC3-II (phagophore and autophagosome bound form). A portion of LC3-II membrane-bound face the cytoplasm and the other face the inner autophagosome and as autophagosome mature and fuse with lysosomes forming autolysosomes, LC3-II is cleaved back to its cytoplasmic form (LC3-I) or is recycled with lysosomal enzymes, respectively [25].

C<sub>2</sub>-ceramide time-dependently increased LC3 lipidation (10 minutes to 24 hours); this time-dependent upregulation or sustained LC3 lipidation was also observed in other cell lines [23, 26]. Thus, suggesting that LC3 lipidation for long periods is an inherent ceramide-induced autophagy mechanism which could reflect a very slow cargo recycling and a slow autophagic compartments turnover. This slow cargo recycling might be the mechanism utilized by ceramide in inducing autophagy-associated cell death or

autophagic cell death. In this scenario, the slow turnover might lead to extensive vacuolization which leads to damage of cellular components and stress build-up with subsequent genomic instability and cell suicide. Yet, this might also suggest that osteoblasts when treated with C<sub>2</sub>-ceramide attempt to survive by activating autophagy, but C<sub>2</sub>-ceramide blocks autophagy leading to stress built up in cells and ultimate cell death.

Moreover, C<sub>2</sub>-ceramide time-dependently increased the formation of autophagosomes and a few autolysosomes or amphisomes (1 and 5 hours) thus, suggesting that the autophagic process is progressing. However, when protease inhibitor was added, most autophagic compartments were double membrane (autophagosomes) containing intact subcellular constituents with the absence of mature single-membrane compartments. Thus, the autophagic process is not progressing. These results confirm that C<sub>2</sub>-ceramide induces fully functioning autophagy in osteoblasts which are blocked by protease inhibitors.

We also investigated the role of Atg5 and beclin1 silencing in C<sub>2</sub>-ceramide induced autophagy-associated cell death in osteoblasts. Silencing both autophagy genes resulted in a significant increase in the percentage of PI-uptake in both MC3T3-E1 cells and POB, thus suggesting a constitutive survival role of Atg5 and beclin1 in osteoblasts. However, in the presence of C<sub>2</sub>-ceramide, the absence of both genes resulted in a significant rescue of the C<sub>2</sub>-ceramide induced cell death in both MC3T3-E1 and POB. Thus, suggesting a C<sub>2</sub>-ceramide stimulated death role of Atg5 and beclin1 in osteoblasts. Consistent with the C<sub>2</sub>-ceramide induced Atg5 and beclin1-dependent cell death in osteoblasts, Park *et al.* [24] reported Atg5-dependent cell death induced by combined treatment with vorinostat and sorafenib in human hepatocellular carcinoma and renal cell carcinoma.

This dual effect of Atg5 and beclin1 in osteoblast could be explained, as Pattingre *et al.* [7] suggested, by a beclin1-Bcl-2 complex that may act as a sensor for the maintenance of autophagy levels within the homeostatic range rather than non-physiological levels that lead to cell death. So, in the absence of ceramide, the binding of beclin-1 by Bcl-2 ensures regulated autophagy (for survival) in response to stimuli. However, C<sub>2</sub>-ceramide might lead to the dissociation of beclin1 from Bcl-2, thus forming free, unchecked beclin-1 that may lead to extensive levels of autophagy with subsequent cell death induction. This ceramide induced dissociation of beclin1 from Bcl-2 has been reported by several investigators. In addition, the basal levels of beclin1 in osteoblasts were relatively high and C<sub>2</sub>-ceramide did not induce a considerable beclin1 upregulation as compared to controls. However, osteoblasts could be very sensitive to minute changes in beclin1 expression which might partly explain the role of beclin1 in the C<sub>2</sub>-ceramide induced osteoblast cell death. Again, the rescue observed by silencing beclin1 although significant, was yet very minimal implicating other effectors in the process. Furthermore, Atg5

has been suggested to play a role in apoptotic cell clearance during PCD [27]. This involvement of Atg5 with PCD is consistent with the role of C<sub>2</sub>-ceramide in inducing Atg5-dependent cell death in osteoblasts. Thus, the C<sub>2</sub>-ceramide-induced Atg5 and beclin1 protein upregulation is possibly part of the C<sub>2</sub>-ceramide-induced cell death pathway in osteoblast, rather than the autophagy pathway.

Our results additionally demonstrated a C<sub>2</sub>-ceramide induced Atg5 and beclin1-independent autophagy in osteoblasts. Consistently, Nishida *et al.* [28] reported the existence of an alternative autophagy pathway that is independent of Atg5. They have shown that etoposide-induced autophagic compartments in *Atg5*<sup>-/-</sup> MEFs (embryonic fibroblasts obtained from *Atg5* knockout mice), thus suggesting the existence of an alternative-non canonical autophagy pathway. Furthermore, analysis of this alternative autophagy during erythrocyte maturation suggested that this alternative pathway may play a role in erythrocyte terminal differentiation. However, this alternative Atg5-dependent autophagy did not induce LC3 lipidation which questions whether this is autophagy in the first place. Yet, in our study, the C<sub>2</sub>-ceramide-induced Atg5 and beclin1-independent autophagy are associated with LC3 lipidation which confirms that what C<sub>2</sub>-ceramide induces alternative autophagy in osteoblasts.

On the other hand, the presence of trace levels of Atg5 and beclin1 proteins, after significantly reducing their levels due to Atg5 and beclin1 siRNA transfection, might be enough to contribute to the C<sub>2</sub>-ceramide induced autophagy. Another possibility is that Atg5 and beclin1 are effectors in the ceramide-induced autophagy but in their absence, ceramide utilizes other pathways in inducing autophagy. In this new pathway, the rate of turnover is quicker as reflected by the presence of more single-membrane mature autophagosomes containing degraded content which might contribute to more resistant osteoblasts to the C<sub>2</sub>-ceramide induced cell death. Thus, this might suggest that C<sub>2</sub>-ceramide induces autophagy with slow turnover in the presence of Atg5 and beclin1. However, in their absence, C<sub>2</sub>-ceramide induces autophagy with a quicker and more efficient turnover to resist cell death. Therefore, further analysis is needed to assess the possibility that C<sub>2</sub>-ceramide induces both canonical and non-canonical autophagy in osteoblasts.

Cumulatively, these data suggest that C<sub>2</sub>-ceramide activates autophagy with the slow flux of cargo from autophagosomes to lysosomes in osteoblasts. This slow turnover, accompanied by extensive cytoplasmic vacuolization, possibly stresses cells and contributes to the apoptotic cell death observed in osteoblasts. Alternatively, C<sub>2</sub>-ceramide-induced autophagy in osteoblasts is a mechanism to ensure the efficient clearance of apoptotic cells as reported by Qu *et al.* [27]. However, quantitative confirmation of these descriptive conclusions is still needed. **Figure 6** depicts a



summary of the proposed mechanisms of C<sub>2</sub>-ceramide-induced autophagy-associated cell death in osteoblasts.

## CONCLUSION

The existence of an alternative autophagy pathway proves that the autophagy process is complicated, and the utilization of such a functional pathway may depend on the stimulus and the type of studied cells. Understanding the molecular events regulating these various pathways could prove useful in the design of drugs for the treatment of various diseases including bone diseases with high turnover such as Paget's disease of bone and osteosarcoma.

**ACKNOWLEDGMENTS:** The authors acknowledge both funding sources for their technical and financial support.

**CONFLICT OF INTEREST:** None

**FINANCIAL SUPPORT:** This project was funded by the Deanship of Scientific Research (DSR) at King Abdulaziz University, Jeddah, Saudi Arabia and the Saudi Cultural Attaché London, UK. Thus, the authors acknowledge both funding sources for their technical and financial support.

**ETHICS STATEMENT:** All work was performed at King's College London in accordance with UK Home Office Project License P8D5E2773 (K.J.L.).

## REFERENCES

- Yorimitsu T, Klionsky DJ. Autophagy: molecular machinery for self-eating. *Cell Death Differ.* 2005;12(2):1542-52.
- He C, Klionsky DJ. Regulation mechanisms and signaling pathways of autophagy. *Annu Rev Genet.* 2009;43:67-93.
- Hara T, Nakamura K, Matsui M, Yamamoto A, Nakahara Y, Suzuki-Migishima R, et al. Suppression of basal autophagy in neural cells causes neurodegenerative disease in mice. *Nature.* 2006;441(7095):885-9.
- Komatsu M, Waguri S, Chiba T, Murata S, Iwata JI, Tanida I, et al. Loss of autophagy in the central nervous system causes neurodegeneration in mice. *Nature.* 2006;441(7095):880-4.
- Kuma A, Hatano M, Matsui M, Yamamoto A, Nakaya H, Yoshimori T, et al. The role of autophagy during the early neonatal starvation period. *Nature.* 2004;432(7020):1032-6.
- Berry DL, Baehrecke EH. Growth arrest and autophagy are required for salivary gland cell degradation in *Drosophila*. *Cell.* 2007;131(6):1137-48.
- Pattingre S, Bauvy C, Carpentier S, Levade T, Levine B, Codogno P. Role of JNK1-dependent Bcl-2 phosphorylation in ceramide-induced macroautophagy. *J Biol Chem.* 2009;284(5):2719-28.
- Shimizu S, Kanaseki T, Mizushima N, Mizuta T, Arakawa-Kobayashi S, Thompson CB, et al. Role of Bcl-2 family proteins in a non-apoptotic programmed cell death dependent on autophagy genes. *Nat Cell Biol.* 2004;6(12):1221-8.
- Yu L, Alva A, Su H, Dutt P, Freundt E, Welsh S, et al. Regulation of an ATG7-beclin 1 program of autophagic cell death by caspase-8. *Science.* 2004;304(5676):1500-2.
- Settembre C, Annunziata I, Spampinato C, Zaccaro D, Cobellis G, Nusco E, et al. Systemic inflammation and neurodegeneration in a mouse model of multiple sulfatase deficiency. *Proc Natl Acad Sci.* 2007;104(11):4506-11.
- Settembre C, Artega-Solis E, Ballabio A, Karsenty G. Self-eating in skeletal development: implications for lysosomal storage disorders. *Autophagy.* 2009;5(2):228-9.
- Bohensky J, Shapiro IM, Leshinsky S, Terkhorn SP, Adams CS, Srinivas V. HIF-1 regulation of chondrocyte apoptosis: induction of the autophagic pathway. *Autophagy.* 2007;3(3):207-14.
- Helfrich MH, Hocking LJ. Genetics and aetiology of Pagetic disorders of bone. *Arch Biochem Biophys.* 2008;473(2):172-82.
- Meschini S, Condello M, Calcabrini A, Marra M, Formisano G, Lista P, et al. The plant alkaloid voacamine induces apoptosis-independent autophagic cell death on both sensitive and multidrug resistant human osteosarcoma cells. *Autophagy.* 2008;4(8):1020-33.
- Komatsu M, Waguri S, Koike M, Sou YS, Ueno T, Hara T, et al. Homeostatic levels of p62 control cytoplasmic inclusion body formation in autophagy-deficient mice. *Cell.* 2007;131(6):1149-63.
- Pandey S, Murphy RF, Agrawal DK. Recent advances in the immunobiology of ceramide. *Exp Mol Pathol.* 2007;82(3):298-309.
- Lavie G, Scarlatti F, Sala G, Levade T, Ghidoni R, Botti J, et al. Is autophagy the key mechanism by which the sphingolipid rheostat controls the cell fate decision?. *Autophagy.* 2007;3(1):45-7.
- Scarlatti F, Bauvy C, Ventruti A, Sala G, Cluzeaud F, Vandewalle A, et al. Ceramide-mediated macroautophagy involves inhibition of protein kinase B and up-regulation of beclin 1. *J Biol Chem.* 2004;279(18):18384-91.
- Sudo H, Kodama HA, Amagai Y, Yamamoto S, Kasai S. In vitro differentiation and calcification in a new clonal osteogenic cell line derived from newborn mouse calvaria. *J Cell Biol.* 1983;96(1):191-8.
- Heath JK, Atkinson SJ, Meikle MC, Reynolds JJ. Mouse osteoblasts synthesize collagenase in response to bone resorbing agents. *Biochim Biophys Acta Gen Subj.* 1984;802(1):151-4.
- Boya P, González-Polo RA, Casares N, Perfettini JL, Dessen P, Larochette N, et al. Inhibition of macroautophagy triggers apoptosis. *Mol Cell Biol.* 2005;25(3):1025-40.
- Liang XH, Jackson S, Seaman M, Brown K, Kempkes B, Hibshoosh H, et al. Induction of autophagy and inhibition of tumorigenesis by beclin 1. *Nature.* 1999;402(6762):672-6.
- Daido S, Kanzawa T, Yamamoto A, Takeuchi H, Kondo Y, Kondo S. Pivotal role of the cell death factor BNIP3 in ceramide-induced autophagic cell death in malignant glioma cells. *Cancer Res.* 2004;64(12):4286-93.
- Park MA, Zhang G, Martin AP, Hamed H, Mitchell C, Hylemon PB, et al. Vorinostat and sorafenib increase ER stress, autophagy and apoptosis via ceramide-dependent CD95 and PERK activation. *Cancer Biol Ther.* 2008;7(10):1648-62.
- Sou YS, Waguri S, Iwata JI, Ueno T, Fujimura T, Hara T, et al. The Atg8 conjugation system is indispensable for proper development of autophagic isolation membranes in mice. *Mol Biol Cell.* 2008;19(11):4762-75.
- Li DD, Wang LL, Deng R, Tang J, Shen Y, Guo JF, et al. The pivotal role of c-Jun NH2-terminal kinase-mediated Beclin 1 expression during anticancer agents-induced autophagy in cancer cells. *Oncogene.* 2009;28(6):886-98.
- Qu X, Zou Z, Sun Q, Luby-Phelps K, Cheng P, Hogan RN, et al. Autophagy gene-dependent clearance of apoptotic cells during embryonic development. *Cell.* 2007;128(5):931-46.
- Nishida Y, Arakawa S, Fujitani K, Yamaguchi H, Mizuta T, Kanaseki T, et al. Discovery of Atg5/Atg7-independent alternative macroautophagy. *Nature.* 2009;461(7264):654-8.